Determinants of electronic waste generation in Bitcoin network: Evidence from the machine learning approach

Determinants of electronic waste generation in Bitcoin network: Evidence from the machine learning approach

Rabin K. Jana[a], Indranil Ghosh[b], Debojyoti Das[c], Anupam Dutta[d]*

a. Operations & Quantitative Methods Area, Indian Institute of Management Raipur, Atal Nagar, Chhattisgarh, India

b. IT & Analytics Area, Institute of Management Technology Hyderabad, Shamshabad, Hyderabad-501218, Telangana, India

c. Finance & Accounting Area, Indian Institute of Management Bangalore, Bengaluru, Karnataka, India

d. School of Accounting and Finance, University of Vaasa, Vaasa, Finland

---

*Corresponding author

{a.rkjana@iimraipur.ac.in; b. indranil@imthyderabad.ac.in; c.debojyoti.das@iimb.ac.in; d.adutta@uwasa.fi}

ORCID: 0000-0001-8564-112X (Rabin K. Jana)

Determinants of electronic waste generation in Bitcoin network: Evidence from the machine learning approach

Abstract

Electronic waste is generating in the Bitcoin network at an alarming rate. This study identifies the determinants of electronic waste generation in the Bitcoin network using machine learning algorithms. We model the evolutionary patterns of electronic waste and carry out a predictive analytics exercise to achieve this objective. The Maximal Information Coefficient (MIC) and Generalized Mean Information Coefficient (GMIC) help to study the association structure. A series of six state-of-the-art machine learning algorithms - Gradient Boosting (GB), Regularized Random Forest (RRF), Bagging-Multiple Adaptive Regression Splines (BM), Hybrid Neuro Fuzzy Inference Systems (HYFIS), Self-Organizing Map (SOM), and Quantile Regression Neural Network (QRNN) are used separately for predictive modeling. We compare the predictive performance of all the algorithms. Statistically, the GB is a superior model followed by RRF. The performance of SOM is the least accurate. Our findings reveal that the blockchain's size, energy consumption, and the historical number of Bitcoin are the most determinants of electronic waste generation in the Bitcoin network. The overall findings bring out exciting insights into practical relevance for effectively curbing electronic waste accumulation.

Keywords: Bitcoin; Blockchain; Electronic Waste; Non-parametric Statistics; Machine Learning

1. Introduction

Bitcoin enables peer-to-peer financial transaction processing bypassing the monitoring of centralized institutions (Nakamoto, 2008). Bitcoin's efficacy in transactional easiness, trust, and security has allured traders in bitcoin mining to earn a high quantum of profit. Bitcoin processing's underlying backbone is the blockchain that acts as a cryptographically secured distributed ledger responsible for recording transactions. The Bitcoin mining process involves verifying transactions through the addition of new blocks traversing across the blockchain network and rewarding the block's creator with new coins reflecting the profit (Das and Dutta, 2020; Greenberg and Bugden, 2019). Consequently, blockchain is identified as a strategic technological innovation that has remarkably revolutionized monetary transactions and digital commodity exchanges (Aggarwal et al., 2019; Di Silvestre et al., 2020). However, a severe problem in the form of accumulation of electronic waste owing to the Bitcoin mining process with advanced hardware and machinery is observed of late (De Vries, 2019). Electronic waste generation can be extremely hazardous with severe implications.

The operational steps of Bitcoin mining hosted in a blockchain network are computationally complex and expensive. The proof-of-work algorithm, representing a cryptographic puzzle, is executed for verifying the transaction and generating Bitcoin. The process is enormously expensive in terms of computation and demands the usage of high-end systems. Escalating Bitcoin demand results in more users foray into competition. Consequently, the competitive network further toughens the mining process (Islam et al., 2019). So, the miners prefer to opt for high-end sophisticated hardware and machinery (Kristoufek, 2020). The introduction of new machines and growing hash rates force the less

effective systems and hardware to phase out at an increasing pace (De Vries, 2019; Li et al., 2019) and result in a tremendous surge in the piling up of electronic waste. Overall, several countries' electronic waste generation in a year is comparable with the electronic waste of the Bitcoin network in the same period. Figure 1 shows that one Bitcoin transaction creates approximately 109 grams of electronic waste. Besides, Figure 2 illustrates that Bitcoin's electronic waste footprint is significantly more than the electronic waste footprint of financial organizations like VISA and other household commodity items.

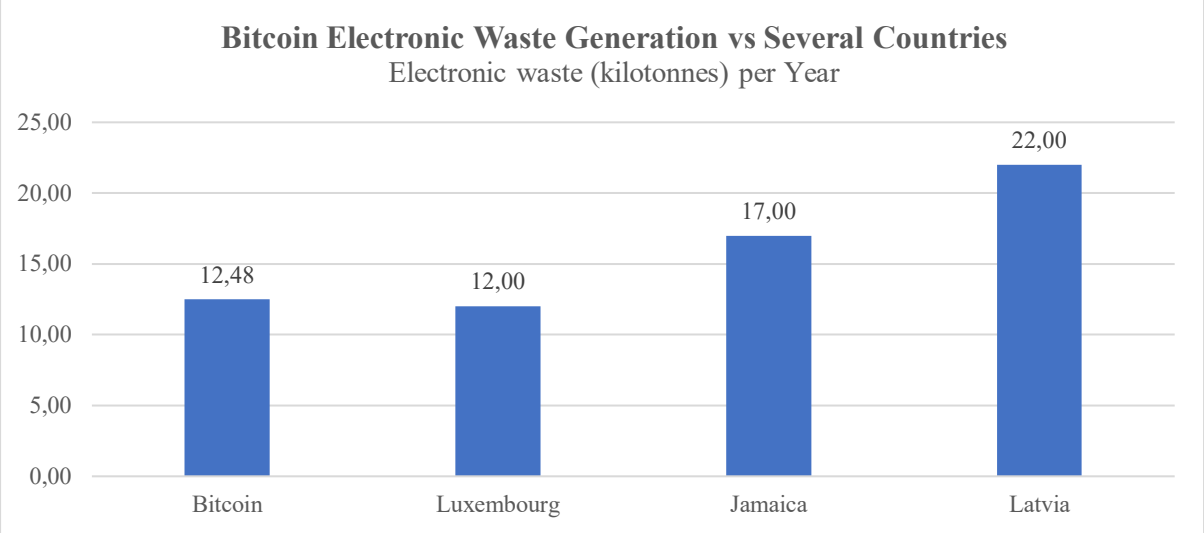

Figure 1. Electronic waste generation by Bitcoin and other countries
Note: Figure 1 exhibits a comparative representation of annual electronic waste generated by Bitcoin and several other countries. The data is sourced from Digiconomist (available at: https://digiconomist.net/bitcoin-electronic-waste-monitor/).

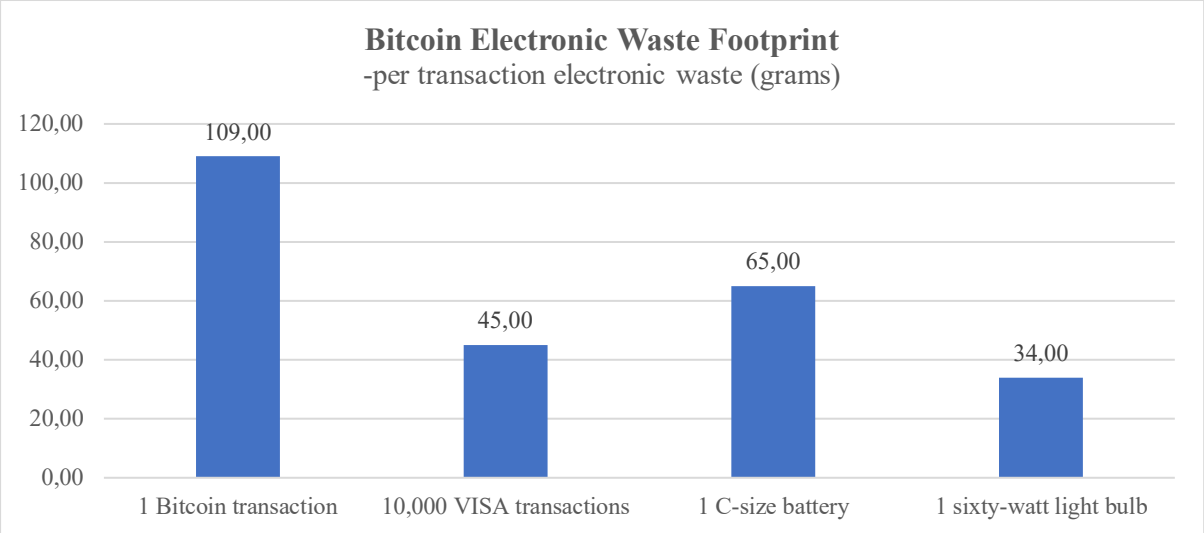

Figure 2. Comparative representation of electronic waste footprint
Note: Figure 2 illustrates a comparative depiction of the electronic waste footprint of a single Bitcoin transaction with respect to the quantum of electronic wastes generated from common household items and 10,000 transactions in well-known financial institutions like VISA. The data is sourced from Digiconomist (available at: https://digiconomist.net/bitcoin-electronic-waste-monitor/).

The mining hardware manufacturers develop state-of-the-art hardware architecture for accelerating computation speed to fasten mining operations (Duong et al., 2020). The advanced mining devices immediately replace the existent cost-inefficient devices. Since these machines are designed on the principle of specificity, it cannot perform beyond the exclusive purpose of mining. Hence, the obsolete mining devices stand out as electronic waste immediately.[1] Lally et al., (2019) posit that the environmental externalities of mining Bitcoin is discussed marginally in the existing literature. Unfortunately, very little attention is paid on the modeling of electronic waste in the Bitcoin network. To the best of our knowledge, no work has been done to identify the factors responsible for accumulating electronic waste and establishing a predictive modeling framework. There is a shortage of research dedicated to modeling electronic waste and identifying its critical drivers for developing predictive modeling. It is necessary to estimate the footprint of electronic waste accumulation daily in the Bitcoin network beforehand. In this research, we resort to state-of-the-art machine learning algorithms to identify the potential contributors of electronic waste linked to bitcoin microstructure by critically expanding the interaction at deeper granules and performing predictive analysis. The above exercises help to draw key insights to combat electronic waste stacking and reduce the hazardous impact.

The contributions of this paper are two folds. First, we identify the key features pertinent to the Bitcoin network leading to electronic waste generation. The degree of association between the considered features and electronic waste is measured. The MIC and GMIC statistics are used in a non-parametric framework to detect complex interrelationships. Second, we carry out predictive modeling of electronic waste to fine-tune blockchain microstructure operations and control electronic waste generation. We use machine learning algorithms like GB, RRF, BM, HYFIS, SOM, and QRNN for this purpose. A comparative performance assessment identifies the best predictive algorithm. The importance scores of the respective independent features are estimated. The predictive exercise's insights are of major practical implications as the findings identify the significant determinants for controlling electronic waste generation. Forecasting future electronic waste trends would also benefit the policymakers for framing strategies for mitigating the negative impacts.

The rest of the paper is structured as follows. We discuss data, their sources, salient features of underlying variables, and fundamental statistical properties in Section 2. Section 3 elaborates on the different components of the research methodology. Section 4 reports the results. Finally, Section 5 concludes the paper by highlighting the key findings, practical implications, limitations, and future research directions.

2. Data description

Daily data of Bitcoin's electronic waste and ten market microstructure variables ranging from February 10, 2017, to May 14, 2020, have been compiled for research modeling. Two dedicated data repositories, namely, www.quandl.com and www.digiconomist.net have been chosen for extracting the variables. Both data sources have been acknowledged to serve reliable information in the scientific literature (De Vries, 2019) and collate real-time daily data. The said data repositories help to conduct mainstream research for drawing actionable insights (Das and Dutta, 2020). The dataset has practical relevance in building an empirical model to recognize the inherent patterns of hazardous impacts. Das and Dutta (2020) model the empirical interplay of energy consumption and miners' revenue of Bitcoin mining using the

[1] Digiconomist, "Bitcoin Electronic Waste Monitor". Available at: https://digiconomist.net/bitcoin-electronic-waste-monitor/, accessed 10-05-2021, 21:10, IST.

available data from the same sources. Table 1 provides a brief outline of the considered variables and their sources. Figure 3 presents the temporal evolutionary patterns of the respective variables under consideration. Table 2 reports descriptive statistics of the regarded series.

Table 1. Variable description

Variable	Description	Source
Electronic waste (Ewaste)	This variable represents the quantity of electronic waste generated by the Bitcoin network in Kilotonnes per year.	Digiconomist
Energy Consumption (Energy)	Energy consumption reflects the quantum of energy discharged in daily Bitcoin mining operations measured in Terawatt–Hours (TwH).	Digiconomist
Average Block Size (Bitcoin_Block)	The size of blocks in the Bitcoin blockchain governs transaction capabilities. A larger block size demands higher computational time. Thus, the probability of creating the quantum of electronic waste is directly influenced by block size. Hence, we have considered an average block size as an explanatory construct here.	Quandl
Blockchain Size (Bitcoin_Blockchain)	The daily increase of blockchain size is a critical indicator of electronic waste, which measures the total size of all block headers and transactions.	Quandl
Transaction Cost (Transaction_Cost)	Expresses miner's revenue divided by the number of transactions.	Quandl
Hash Rate (Bitcoin_Hashrate)	The hash rate simply accounts for the number of hashes performed by the Bitcoin network per second.	Quandl
Miner Revenue (Miner_Revenue)	Miner revenue is estimated as (number of Bitcoins mined per day + transaction fees) * market price.	Quandl
Market Price of Bitcoin (Bitcoin_Marketprice)	Price of Bitcoin in USD.	Quandl
Transactions per block (Transaction_Block)	The number of transactions per block denotes the average number of transactions executed in each block.	Quandl
Bitcoins Mined Per Day (Bitcoin_MinedDay)	Total Bitcoin expresses the historically total number of Bitcoins mined per day.	Quandl
Transaction Fee (Transaction_Fee)	It accounts for the aggregate Bitcoin value of transaction fees miners earn daily.	Quandl

Note: Table 1 describes the variables under consideration. The first column reports all the variable names with the nomenclature in parenthesis. The second column defines the underlying variables in brief. The last column indicates the respective data sources.

The rationale behind choosing the ten variables for predicting Ewaste lies in a careful selection of key contributors linked to Bitcoin mining microstructure, process parameters, and market state. Bitcoin_Block, Bitcoin_Blockchain, and Bitcoin_Hashrate account for the microstructure. Transaction_Cost, Miner_Revenue, Transaction_Block, Bitcoin_MinedDay, and Transaction_Fee are features pertinent to the key process parameters. Bitcoin_Marketprice is the feature that captures the current market value of Bitcoin. To the best of our knowledge, no work reports a systematic approach to identify the key enablers responsible for the surge in electronic waste for Bitcoin mining. Therefore, it is challenging to select and collate necessary

data for building a predictive model for the said purpose. Based on a handful of literature (Rehman and Kang, 2020; De Vries, 2021) dedicated to mining dynamics of blockchain for Bitcoin, we select the ten indicators to estimate Ewaste.

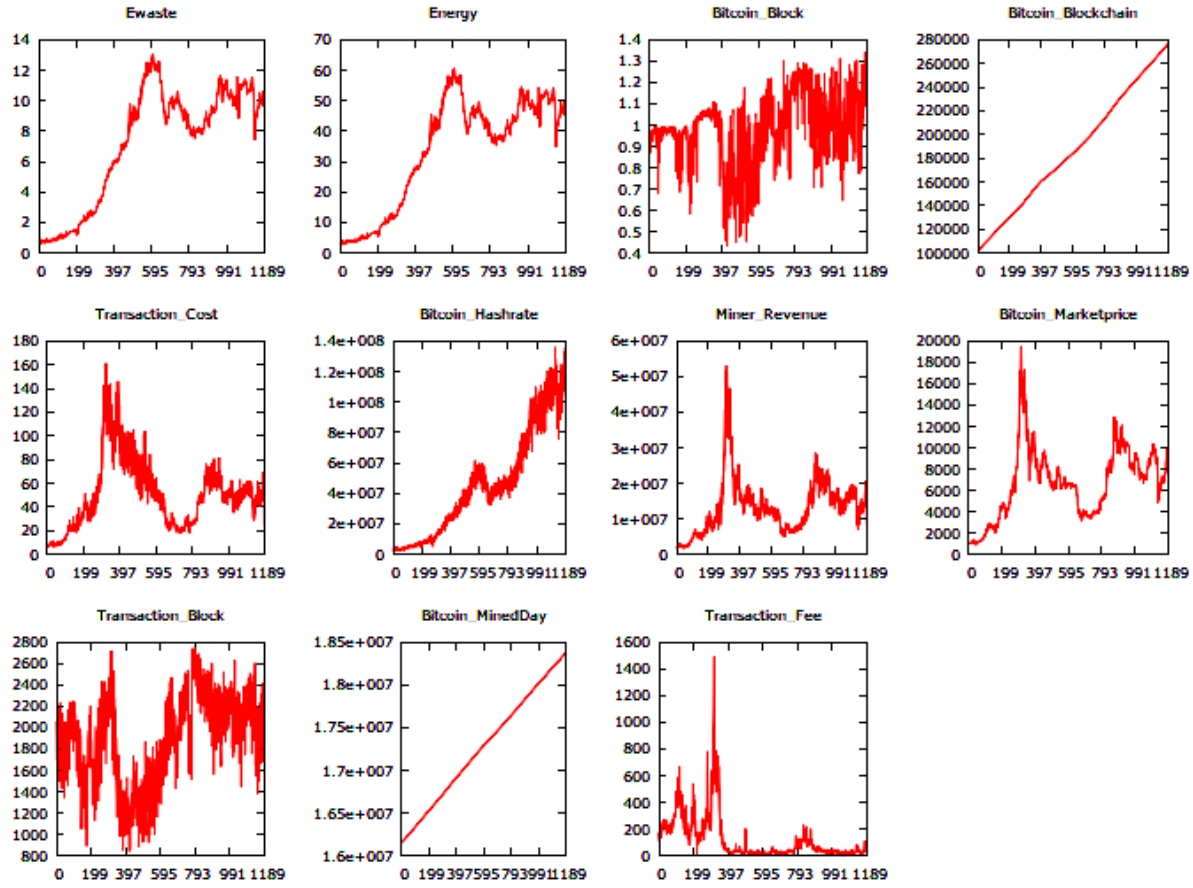

Figure 3. Evolutionary patterns of the underlying variables

Note: Figure 1 depicts the temporal evolutionary patterns of the respective variables under consideration from February 10, 2017, to May 14, 2020.

Table 2. Descriptive statistics

Series	Minimum	Maximum	Mean	Median	Std. Dev.	Skewness	Kurtosis
Ewaste	0.653	12.977	7.141	8.676	3.863	-0.507	-1.232
Energy	3.031	60.252	33.356	40.518	18.07685	-0.510	-1.242
Bitcoin_Block	0.432	1.342	0.986	0.989	0.163	-0.516	0.364
Bitcoin_Blockchain	1018	277138	187229	184147	50117	0.0752	-1.157
Transaction_Cost	6.437	161.686	49.372	47.308	28.432	0.960	1.029
Bitcoin_Hashrate	2917084	136264980	45796689	42003662	35299609	0.621	-0.688
Miner_Revenue	1696707	53191582	13338716	12945905	7846796	1.540	4.331
Bitcoin_Marketprice	941.900	19498.700	6684.800	6733.900	3300.170	0.439	0.509
Transaction_Block	834.100	2762.500	1896.600	1958.800	413.671	-0.365	-0.687
Bitcoin_MinedDay	16154200	18376762	17276722	17292075	642972.700	-0.027	-1.191
Transaction_Fee	9.971	1495.947	122.317	38.978	163.927	2.601	9.343

Note: Table 2 exhibits the descriptive properties of the underlying variables at the level.

Table 3 reports the outcome of statistical tests to ascertain the fundamental characteristics of the mentioned features. Through Shapiro-Wilk and Jarque-Bera tests, normality checks imply that the underlying variables do not abide by the normality assumption. The outcome of the ADF and ERS unit root tests indicates that electronic waste is strictly non-stationary. Thus, two prominent non-parametric and non-stationary behavioral traits emerge. So, orthodox econometric and time series modeling approaches cannot capture inherent associations and execute the predictive analysis. The estimated Hurst exponent values for all series are substantially higher than 0.5. Thus, there is a strong presence of persistent trends and suggests volatility clustering in daily observations of the declared variables. Deploying statistical frameworks tailor-made for delving linear interplay would not be appropriate for electronic waste modeling. Therefore, deployment of MIC and GMIC statistics and advanced machine learning algorithms for decoding the interaction and predictive analytics tasks is rationalized.

Table 3. The outcome of the statistical tests conducted to ascertain data characteristics

Series	Shapiro-Wilk Test	Jarque-Bera Test	ADF Test	ERF Test	Hurst Exponent
Ewaste	0.879***	126.050***	0.485#	0.299#	0.915
Energy	0.877***	127.880***	0.491#	0.306#	0.905
Bitcoin_Block	0.976***	59.027***	-1.563#	-1.598#	0.726
Bitcoin_Blockchain	0.957***	67.414***	16.108#	2.981#	0.938
Transaction_Cost	0.937***	233.670***	-2.083**	-1.988**	0.814
Bitcoin_Hashrate	0.913***	99.938***	-0.587#	1.276#	0.674
Miner_Revenue	0.890***	1388.500***	-1.440#	-1.211#	0.720
Bitcoin_Marketpric	0.971***	50.629***	-0.452#	-0.628#	0.895
Transaction_Block	0.974***	49.856***	-1.540#	-1.591#	0.775
Bitcoin_MinedDay	0.955***	70.387***	27.797#	1.131#	0.938
Transaction_Fee	0.676***	5620.200***	-3.587***	-2.824***	0.825

Note: *** Significant at 1% level of significance, ** Significant at 5% level of significance, # Not Significant, ADF Test: Augmented Dickey-Fuller Test, ERS Test: Elliot Rothenberg and Stock Test

3. Research Methodology

The nexus between Bitcoin's electronic waste and ten market microstructure variables is delved into, and a predictive modeling exercise is carried out to accomplish the research objectives. This research deploys six machine learning driven predictive analytics algorithms - GB, RRF, BM, HYFIS, SSOM, and QRNN. These algorithms belong to two broad strands, namely, ensemble machine learning and neural modeling of machine learning with equal proportion. The GB, RRF, and BM belong to the ensemble machine learning class, while HYFIS, SSOM, and QRNN belong to neural modeling of the machine learning class. As GB, RRF, and BM are the advanced variants of three major ensemble machine learning, and three neural modeling techniques are chosen to keep a balance for comparing the results. Thus, the selection of predictive models effectively assists in comparing two major classes of machine learning algorithms. In this section, we briefly enunciate the techniques deployed for implementing the tasks.

3.1 Association mining

We utilize MIC and GMIC for mining the pairwise interplay between the electronic waste and independent features. The estimated values of MIC and GMIC provide the importance of the respective features.

3.1.1 Maximal information coefficient (MIC)

The MIC was conceptualized and developed by Reshef et al. (2011) for measuring the prevailing linear or nonlinear bivariate association. It is like the orthodox coefficient of regression (R^2) with additional capabilities of detecting nonlinear nexus. The MIC belongs to the maximal information-based nonparametric exploration (MINE) class of statistics for evaluating dynamic interdependence. MIC statistic varies between 0 to 1 where 0 indicates independence, and 1 denotes perfect association.

3.1.2 Generalized mean information coefficient (GMIC)

The GMIC (Luedtke & Tran, 2013) addresses some reported shortcomings of MIC in the presence of high noise components. It belongs to the MINE family of statistics capable of extracting the association of functional and non-functional forms. Likewise, MIC, GMIC values range between 0 to 1. Thus, a combination of GMIC and MIC statistics would be capable of mining relationships manifested by the superimposition of functions and other forms of complex nonlinear structures.

3.2 Predictive modeling

Association mining is followed by multivariate predictive analytics exercise of electronic waste of Bitcoin blockchain. The paper utilizes six machine learning algorithms - RRF, GB, BM, HYFIS, SOM, and QRNN. RRF, GB, and BM belong to the ensemble machine learning category, while HYFIS, SOM, and QRNN are advanced forms of neural network-based machine learning. Thus, this work tests two distinct categories of machine learning algorithms in the prediction task. We assess the predictive performance of individual models and statistically compare the performance evaluation to identify the most suitable model. The predictive analysis provides sufficient evidence on whether electronic waste in blockchain can be estimated using the selected features or not. We outline the working principles of individual models.

3.2.1 Gradient boosting (GB)

GB is a variant of the popular boosting algorithm developed by Schapire & Singer (1999) to perform ensemble machine learning for predictive analysis. A series of different learning algorithms are utilized sequentially in a forward-stage wise direction to estimate final forecasts. GB implements the boosting framework by estimating the gradient driver residual to identify samples on which predictive performance is weak. We use classical regression trees for predictive modeling in the forward direction at each phase of sequential learning. The fundamental operational steps of the GB algorithm remain the same as of boosting that are narrated below:

Step 1: Initialize each sample's weight to 1/e, where e is the cardinality of set E and N training samples belong to set E.
Step 2: For individual base learners (i) execute the following subtasks.

2.1: Bootstrapped samples are extracted to form a new training set, D_i.
2.2: Deploy the generated set D_i for the training process of model M_t.
2.3: Estimate the residual of M_t ($Err(M_t)$).
2.4: If the estimated residual emerges to be greater than 0.5, repeat steps 2.1 to 2.3 or execute step 2.5.
2.5: Update weights for elements of D_i.
2.6: Normalize the weight vector.

Step 3: Calculate the degree of accuracy of respective base learners.
Step 4: Output of respective base learners are eventually aggregated to draw the result.

Scikit-learn library in python has been utilized for implementing the model.

3.2.2 Regularized random forest (RRF)

RRF (Deng & Runger, 2013) helps to tackle feature selection problems. It is an ensemble machine learning algorithm and used for predictive modeling purposes. The algorithm is similar to an orthodox random forest algorithm. Trees are grown using bootstrapped samples. The difference lies in compact feature selection, which attempts to boost the performance of RRF. To identify the most suitable feature for splitting operations at each node of constituent decision trees, the regularized information gain ($Gain_R(X_i, v)$) of a feature (X_i) for splitting node v is estimated as:

$$Gain_R(X_i, v) = \begin{cases} \lambda . Gain(X_i, v) & i \notin F \\ Gain(X_i, v) & i \in F \end{cases} \quad (1)$$

where $$Gain(X_i, v) = Gini(X_i, v) - w_L Gini(X_i, v^L) - w_R Gini(X_i, v^R) \quad (2)$$

where v^L and v^R are the left and right child nodes of node v, F set of indices of features, and w_L, w_R denote the number of cases assigned to both nodes. The parameter $\lambda \in (0,1]$ denotes the penalty coefficient. RRF is extremely useful in identifying the best features for splitting operations. In this work, we use 'RRF' package of R for simulating the RRF algorithm.

3.2.3 Bagging-MARS (BM)

BM is a combination of Bagging and MARS for predictive modeling. Like GB, bagging (Bootstrap Aggregating) is also an ensemble machine learning algorithm. BM is fundamentally different from GB in the operational process as it achieves an ensemble structure by utilizing a series of base learners in parallel (Simidjievski et al., 2015). The final prediction is estimating by the averaging outcome of individual base classifiers built on bootstrapped samples. If there are n number of base learners, then the Bagging outcome is obtained using equation (3).

$$y(x) = \frac{1}{n}\sum_{i=1}^{n} y_i(x) \quad (3)$$

where $y_i(x)$ is the outcome of i^{th} learner.

In BM, the MARS algorithm (Friedman, 1991) acts as a base learner. MARS mimics stepwise linear regression to effectively model complex relationships. It fits a series of linear regressions on different intervals of the independent variable(s) associated with a problem to delve into complicated relationships critically. The MARS algorithm's key challenge is to estimate the appropriate intervals to apply linear regression models independently. MARS

utilizes a series of basis functions by mapping the original variables to newer ones to develop a predictive model with piecewise linear regression splines. Interactions among the basis functions express interactions among the independent variables. These basis functions are comprised of reflected pairs for individual input variables (x_j) with knots at each observed value (x_{ij}) of that variable, shown in equation (4).

$$C = \{(x_j - t)_+, (t - x_j)_+\} \tag{4}$$

where $t \in \{x_{1j}, x_{2j}, \ldots\ldots, x_{Nj}\}$ and $j = 1, 2, \ldots\ldots, p$.

Equation (5) expresses the general form of MARS as follows:

$$Y = f(X) = \beta_0 + \sum_{m=1}^{M} \beta_m h_m(X) \tag{5}$$

where $h_m(X)$ is a basis function from set C or a product of two or more such functions. We estimate the coefficients by minimizing the residual sum of squares. Basis functions in pairs are added in a greedy manner to fit the data according to the knots. The package 'caret' of R has been invoked for implementing the model.

3.2.4 Hybrid neuro fuzzy inference systems (HYFIS)

HYFIS (Kim and Kasabov, 1999) belongs to the neuro-fuzzy modeling family, like ANFIS and DENFIS (Atsalakis et al., 2019). It combines the fuzzy rule-driven inference framework with an MLP based ANN structure for carrying out predictive modeling tasks. HYFIS comprises five distinct layers utilized for input, fuzzification, rule mining, defuzzification, and output generation process. It adopts a two-phase learning scheme. The first phase, referred to as the knowledge acquisition stage, is responsible for deriving fuzzy rules from training samples. In the second phase, the gradient descent learning framework is deployed for tuning membership functions of input-output linguistic variables. The 'frbs' package of R has been used for testing the model.

3.2.5 Supervised self-organizing map (SSOM)

The SSOM (Kohonen, 1982) mimics the principle of SOM. SOM was designed for performing unsupervised clustering tasks by mapping a high-dimensional input into a lower-dimensional space following the similarity of data points. It can perform regression or classification tasks by treating the target as a special set of variables and proceeding with the training process to create input vectors through the concatenation of the target with appropriate data labels. We use the 'kohonen' package in R for building the model.

3.2.6 Quantile regression neural network (QRNN)

The QRNN model's objective is to estimate predictions at different quantiles using ANN architecture (Cannon, 2011). Although quantile regression is tailor-made for accomplishing the task, it suffers from several shortcomings. The QRNN model can overcome the shortcomings of QR and is based on traditional ANN comprising input, hidden, and output layers.

The output of the hidden layer is estimated as:

$$g_j(t) = tanh\left(\sum_{i=1}^{I} x_i(t) w_{ij}^{(h)} + b_j^{(h)}\right) \quad (6)$$

where $x_i(t)$ and $w_{ij}^{(h)}$ represent inputs and hidden layer weights respectively, $tanh$ refer to a hyperbolic tangent function, and $b_j^{(h)}$ reflects the bias term. The conditional τ-quantile is governed by:

$$\hat{y}_\tau(t) = f\left(\sum_{j=1}^{J} g_j(t) w_j^{(o)} + b^{(o)}\right) \quad (7)$$

where $w_j^{(o)}$ and $b^{(o)}$ denote weights and bias of the output layer, and $f(.)$ is a transfer function of the layer. The selection of transfer function decides whether censor regression quantiles to be determined or not. Package 'qrnn' has been utilized for simulating the model.

We test different packages of R and Python, like 'gbm', 'xgboost', 'ipred', etc., and select packages with superior performance in terms of accuracy for inclusion in the final implementation in this work.

3.3 Predictive performance assessment

To evaluate the predictive performance of respective machine learning algorithms, we have used four different measures outlined below.

3.3.1 Nash-Sutcliffe efficiency (NSE): In a predictive model, NSE is a ratio of the relative strength of residual variance to observations' actual variance. It is expressed as:

$$NSE = 1 - \frac{\sum_{t=1}^{N}\{\hat{Y}_t - Y_t\}^2}{\sum_{i=1}^{N}\{Y_t - \bar{Y}_t\}^2}, \quad (8)$$

The magnitude of NSE varies between - ∞ to 1. High NSE values indicate superior predictive performance.

3.3.2 Index of agreement (IA): IA is defined as:

$$IA = 1 - \frac{\sum_{t=1}^{N}(\hat{Y}_t - Y_t)^2}{\sum_{i=1}^{N}\{|\hat{Y}_t - \bar{Y}_t| + |Y_t - \bar{Y}_t|\}^2} \quad (9)$$

It evaluates the magnitude of error components. An IA value close to 1 indicate superior prediction.

3.3.3 Theil index (TI): TI is estimated as:

$$TI = \frac{\left[\frac{1}{N}\sum_{t=1}^{N}(\hat{Y}_t - Y_t)^2\right]^{1/2}}{\left[\frac{1}{N}\sum_{i=1}^{N}(\hat{Y}_t)^2\right]^{1/2} + \left[\frac{1}{N}\sum_{i=1}^{N}(Y_t)^2\right]^{1/2}} \quad (10)$$

For a superior prediction, TI values should be close to 0.

3.3.4 Directional predictive accuracy (DA): DA is determined as

$$DA = \frac{1}{N}\sum_{t=1}^{N} D_t \, , D_t = \begin{cases} 1, & (Y_{t+1} - Y_t)\left(\hat{Y}_{t+1} - Y_t\right) \geq 0 \\ 0, & Otherwise \end{cases} \quad (11)$$

Directional predictive performance is critical to record as it can measure models' capability to obtain precise futuristic trends in short and long-run duration. A DA values close to 1 signify high accuracy of directional prediction and close to 0 infer inferior directional prediction.

3.4 Comparative performance evaluation

Performing a comparative statistical performance is essential to identify the superior model for practical implications. This study deploys two frameworks, test for equal predictive ability and test for the superior predictive power for achieving the endeavor. Diebold-Mariano (DM) test performs equal predictive ability checks. In contrast, the model confidence set (MCS) test carries out a test of superior predictive ability. If the DM test cannot identify the best model, then MCS is invoked to complete the process. Deployment of DM and MCS driven framework for comparative performance ascertainment in time series forecasting are reported successful (Ghosh et al., 2019; Jana et al., 2020).

4. Results and Discussions

The findings of association analysis and predictive modeling for comprehending the nature of the impact of chosen indicators on electronic waste is presented here.

4.1 Findings of association

We estimate MIC and GMIC coefficients' magnitude by using the *'Minerva'* package of R. Table 4 reports the MIC and GMIC values reflecting the degree of interdependence between the electronic waste and selected features.

We observe that Energy, Bitcoin_Blockchain, and Bitcoin_MinedDay are highly associated with electronic waste as the respective MIC, and GMIC scores are greater than 0.9. Bitcoin_Block, Transaction_cost, Miner_revenue, Transaction_Block share a relatively low association with electronic waste. The findings conform to the outcome of the research of Das & Dutta (2020) that reveals that energy consumption and miner-revenue exhibit negative co-movement in bearish phases. As energy consumption shares a stronger bond with electronic waste, the interdependence of miner-revenue and electronic waste is comparatively weaker. However, the observed MIC and GMIC values imply that all explanatory features exhibit a moderate to a high level of interplay with the target variable. Thus, the overall energy consumptions, size of the blockchain, and the total number of Bitcoins mined per day need comparatively rigorous monitoring compared to other factors to manage the concern of electronic waste.

Table 4. Estimated MIC and GMIC values

Series	MIC	GMIC
Energy	0.999	0.999
Bitcoin_Block	0.427	0.365
Bitcoin_Blockchain	0.999	0.984
Transaction_Cost	0.500	0.460
Bitcoin_Hashrate	0.921	0.907

Miner_Revenue	0.484	0.454
Bitcoin_Marketprice	0.587	0.553
Transaction_Block	0.427	0.346
Bitcoin_MinedDay	0.999	0.984
Transaction_Fee	0.755	0.734

Note: Table 4 reports the Maximal Information Coefficient (MIC) estimated values and Generalized Mean Information Coefficient (GMIC) for the market microstructure variables of Bitcoin.

4.2 Findings of predictive modeling

We use different R and Python packages for conducting predictive modeling. In this exercise, the dataset needs to be segregated into training and test partitions. The present study considers three partitioning schemes. The data set is decomposed into training and test segments of (80-20)%, (70-30)%, and (60-40)% forms. Respective machine learning algorithms have been applied to all these three schemes to assess the accuracy of obtained forecasts. Later, a comparative performance assessment has been used in these three schemes. It must be noted that various process parameters govern all six machine learning algorithms. This work considers ten experimental trials of individual algorithms by varying the process parameters uniformly. The average scores of respective performance indicators are calculated to evaluate predictive ability.

Tables 5-7 report the values of four performance indicators for measuring respective algorithms' performance on different training test data segments.

Table 5. Predictive performance on (80-20)% Setting

	GB	RRF	BM	HYFIS	SSOM	QRNN
			Training Dataset			
NSE	0.999	0.999	0.999	0.999	0.987	0.999
TI	0.000	0.000	0.000	0.000	0.003	0.000
IA	0.999	0.999	0.999	0.999	0.998	0.999
DA	1.000	1.000	1.000	0.992	0.987	0.992
			Test Dataset			
NSE	0.999	0.999	0.999	0.999	0.986	0.999
TI	0.001	0.001	0.002	0.000	0.004	0.002
IA	0.999	0.999	0.999	0.999	0.997	0.999
DA	1.000	1.000	0.992	0.983	0.979	0.983

Table 6. Predictive performance on (70-30)% Setting

	GB	RRF	BM	HYFIS	SSOM	QRNN
			Training Dataset			
NSE	0.999	0.999	0.999	0.999	0.984	0.999
TI	0.001	0.000	0.001	0.001	0.004	0.001
IA	0.999	0.999	0.999	0.999	0.997	0.999

DA	0.989	0.989	0.986	0.983	0.981	0.989
			Test Dataset			
NSE	0.999	0.999	0.998	0.999	0.983	0.998
TI	0.002	0.002	0.003	0.003	0.005	0.003
IA	0.999	0.999	0.999	0.999	0.996	0.999
DA	0.981	0.981	0.981	0.975	0.969	0.981

Table 7. Predictive performance on (60-40)% setting

	GB	RRF	BM	HYFIS	SSOM	QRNN
			Training Dataset			
NSE	0.999	0.999	0.998	0.998	0.982	0.998
TI	0.001	0.001	0.002	0.002	0.021	0.001
IA	0.999	0.999	0.999	0.998	0.996	0.999
DA	0.984	0.985	0.985	0.985	0.978	0.985
			Test Dataset			
NSE	0.999	0.999	0.998	0.997	0.981	0.998
TI	0.008	0.008	0.008	0.009	0.086	0.008
IA	0.999	0.999	0.996	0.993	0.995	0.996
DA	0.981	0.981	0.981	0.978	0.974	0.981

In the (80-20)% scheme, the performance of respective models is sensational as NSE, IA, and DA values are high and TI values are low on training and test data. Among the six algorithms, SOM's performance is marginally less effective, as manifested by respective indicators. Almost the same phenomenon phase prevailed in (70-20)% setting. Finally, the (60-40)% setting reflects circumstances where the presence of historical information may not be abundant. The quality of predictions in this segment would validate the robustness and efficacy of frameworks in modeling electronic waste in extreme cases where historical information availability is restricted. Values of performance indicators, presented in Table 7, imply the loss of precision marginally. However, NSE, TI, IA, and DA's values still lie in the ranges that suggest excellent predictive modeling. So, the proposed multivariate machine learning framework successfully predicts electronic waste quantum using the chosen variables. Thus, any attempt to develop an architecture for controlling the accumulation of electronic waste in the Bitcoin blockchain may benefit from the outcome of predictive modeling. The following Figures 4-9 depict model performances on randomly selected 100 test data.

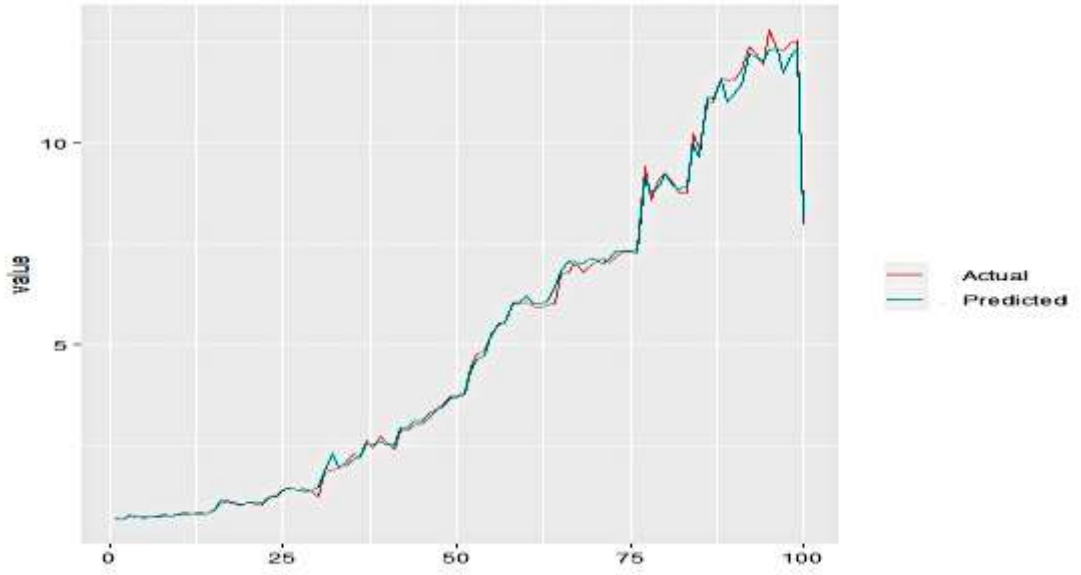

Figure 4. Performance of GB on random test samples of (80-20)% setting

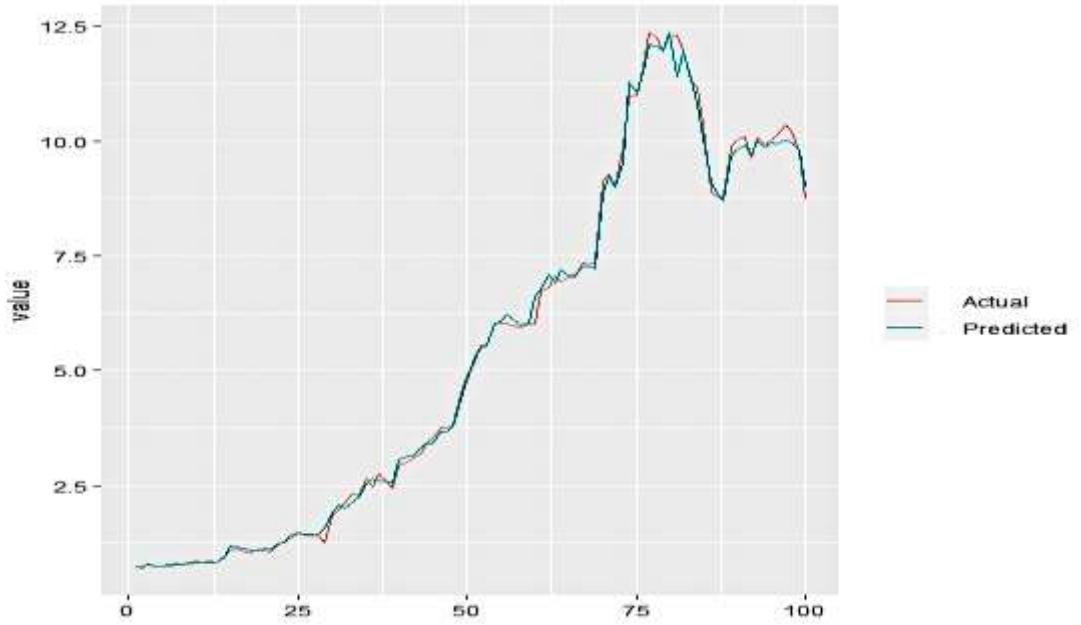

Figure 5. Performance of RRF on a test dataset of (80-20)% setting

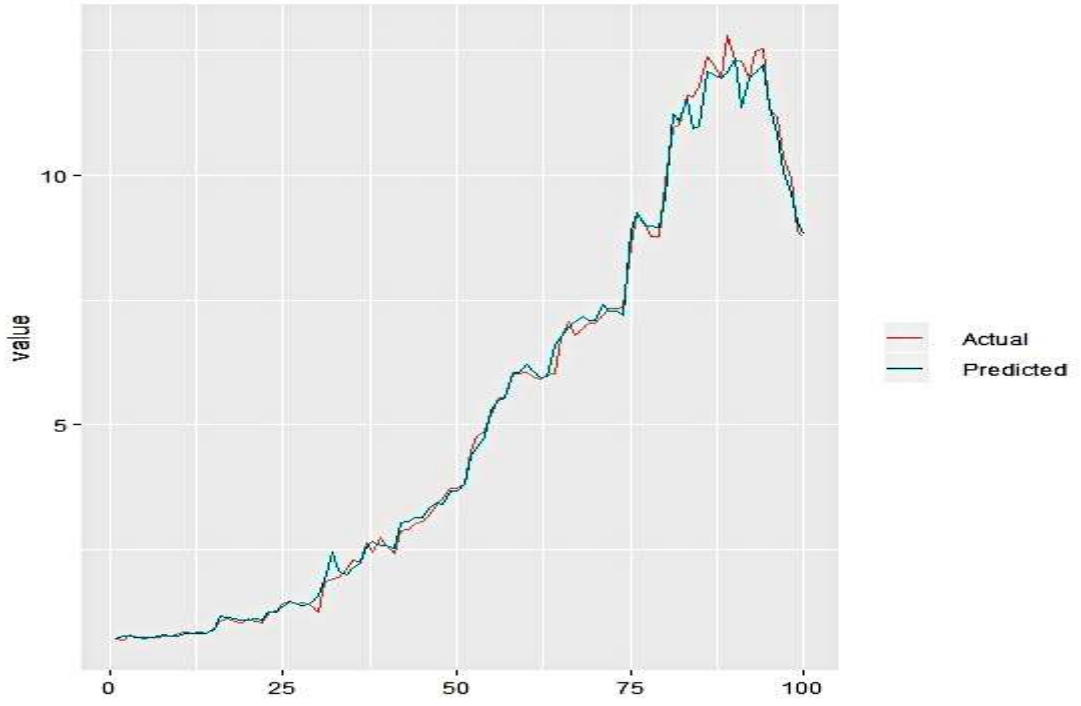

Figure 6. Performance of BM on a test dataset of (80-20)% setting

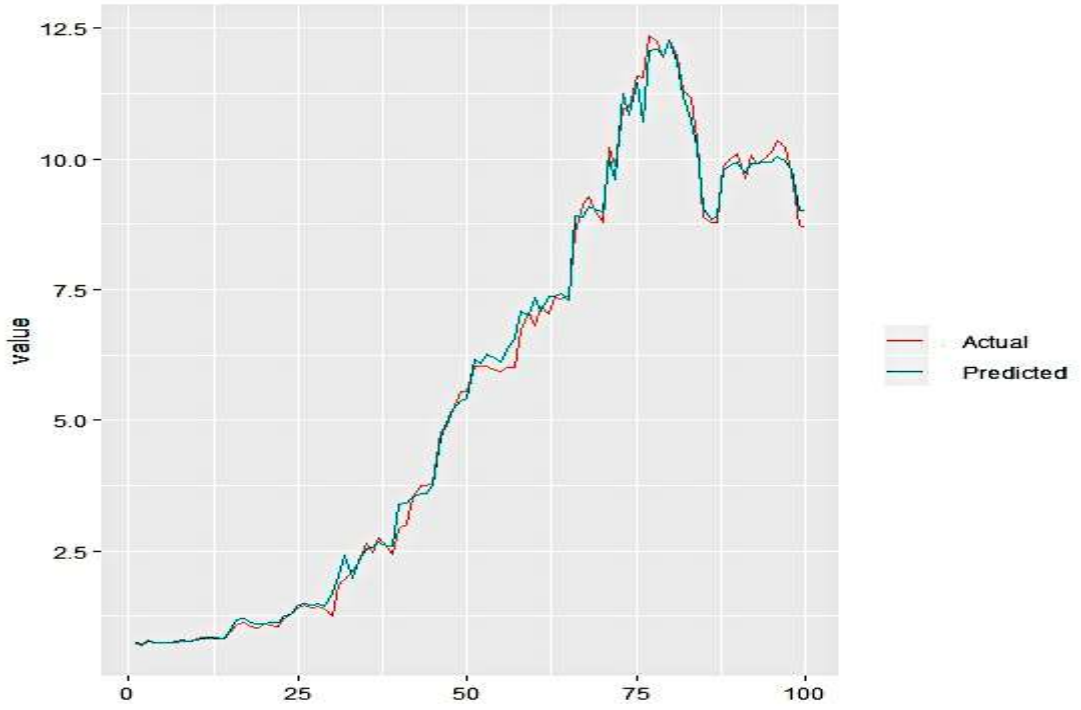

Figure 7. Performance of HYFIS on a test dataset of (80-20)% setting

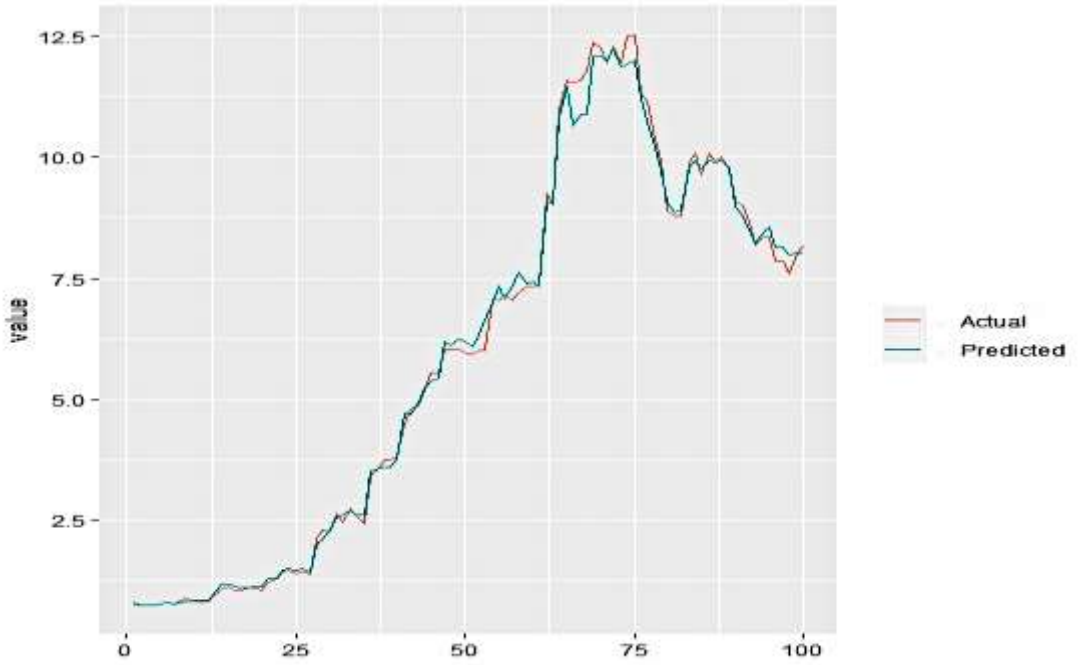

Figure 8. Performance of SOM on a test dataset of (80-20)% setting

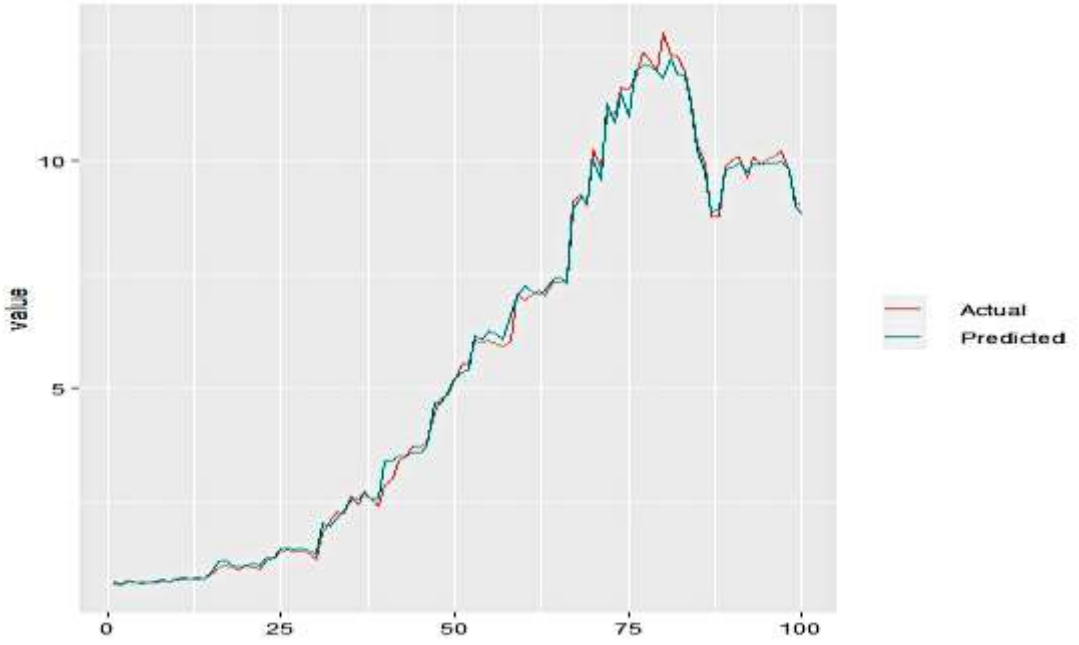

Figure 9. Performance of QRNN on a test dataset of (80-20)% setting

We observe that it is difficult to distinguish between the actual and predicted values that indicate the generation of predictions of supreme precision and supporting the claims made by obtained values of performance indicators.

4.3 A comparative performance evaluation

From the perspective of modeling the temporal dynamics of electronic waste, the predictive analysis segment presented in this paper is extremely effective. However, for

practical deployment purposes, it is necessary to identify the most superior approach. We utilize DM and MCS tests to accomplish the task. Tables 8-10 report the outcome of DM tests. The DM test is a pairwise comparative statistical test for evaluating relative differences in multiple models' performances through mean-squared error measurement. As the test operations are fundamentally guided through paired comparisons, it is essential to set the order of constituents of the pair to eliminate confusion in result interpretations. Orders of models are denoted through an index in parenthesis. For a positively significant test statistic, the second model is better than the first in terms of the predictions' quality. For a negatively significant test statistic, the first model is better than the second one. Lastly, an insignificant test statistic implies no considerable difference in the quality of predictions.

Table 8. DM test on (80-20)% setting

Models	GB (1)	RRF (1)	BM (1)	HYFIS (1)	SSOM (1)	QRNN (1)
GB (2)	-					
RRF (2)	0.231#	-				
BM (2)	0.249#	0.248#	-			
HYFIS (2)	-3.8237***	-3.7684***	0.228#	-		
SSOM (2)	-4.8753***	-4.8647***	-4.7681***	-4.6378***	-	
QRNN (2)	0.237#	0.245#	0.235#	0.228#	-4.7523***	-

Note: *** Significant at 1% level of significance, # Not Significant

Table 9. DM test on (70-30)% setting

Models	GB (1)	RRF (1)	BM (1)	HYFIS (1)	SSOM (1)	QRNN (1)
GB (2)	-					
RRF (2)	0.225#	-				
BM (2)	-3.7962***	-3.7879***	-			
HYFIS (2)	-3.9543***	-3.9436***	0.243#	-		
SSOM (2)	-5.1620***	-5.1207***	-4.8366***	-4.7417***	-	
QRNN (2)	-3.7544***	-3.7368***	0.237#	0.221#	-4.8246***	-

Note: *** Significant at 1% level of significance, # Not Significant

Table 10. DM test on (60-40)% setting

Models	GB (1)	RRF (1)	BM (1)	HYFIS (1)	SSOM (1)	QRNN (1)
GB (2)	-					
RRF (2)	0.216#	-				

BM (2)	-3.8203***	-3.7944***	-			
HYFIS (2)	-3.9611***	-3.9547***	0.241#	-		
SSOM (2)	-5.1694***	-5.2936***	-4.8425***	-4.7494***	-	
QRNN (2)	-3.7623***	-3.7425***	0.235#	0.228#	-4.8310***	-

Note: *** Significant at 1% level of significance, # Not Significant

The outcome of DM tests exhibits an interesting pattern across three settings. It has emerged that no significant differences exist among the performance of GB, RRF, BM, QRNN at (80-20)% dataset. Both GB and RRF outperform HYFIS and SSOM. SSOM's performance is inferior compared to BM, HYFIS, and QRNN. So, at the (80-20)% setting, SSOM is less accurate than the rest. No clear evidence can be drawn to decide the most superior model.

At (70-30)% setting, GB and RRF are statistically superior to other models. No significant difference between the performances of these two models could be found. The performance of SSOM is the most inferior. The predictive ability of BM, HYFIS, and QRF are similar. Thus, no clear evidence can be detected to identify the most superior model in this scheme. A precisely identical outcome has prevailed in (60-40)% setting. GB and RRF statistically outperformed the rest, while SSOM is the least superior. No concrete evidence for identifying the most suitable model could be found. Hence, among the six models, SSOM is comparatively not as good as the other models. In terms of the quality of predictions, SSOM cannot be classified as a flawed model by any means. As the equal predictive ability test paradigm fails to select the most superior model, the MCS approach is invoked, discarding SSOM for comparison. The corresponding results are presented in Table 11.

Table 11. MCS evaluation

Set Up	GB	RRF	BM	HYFIS	QRNN (1)
80-20	(1)	(2)	(4)	(5)	(3)
70-30	(1)	(2)	(4)	(5)	(3)
60-40	(1)	(2)	(3)	(5)	(4)

Note: Table 10 shows the model confidence set (MCS) of the several alternative models used in the study. The results suggest the performance of Gradient Boosting (GB) is superior to others.

The output of the MCS evaluation suggests that GB's performance is the most superior across all the data settings, followed by RRF. Predictions achieved by HYFIS among these five models across all the schemes are comparatively least accurate. As GB has produced predictions of supreme accuracy, it should capture the interrelationship between electronic waste and the chosen explanatory at a deeper level. The inbuilt feature evaluation ability of GB is invoked to determine the relative importance of explanatory features. Figure 10 depicts the result of the feature importance assessment.

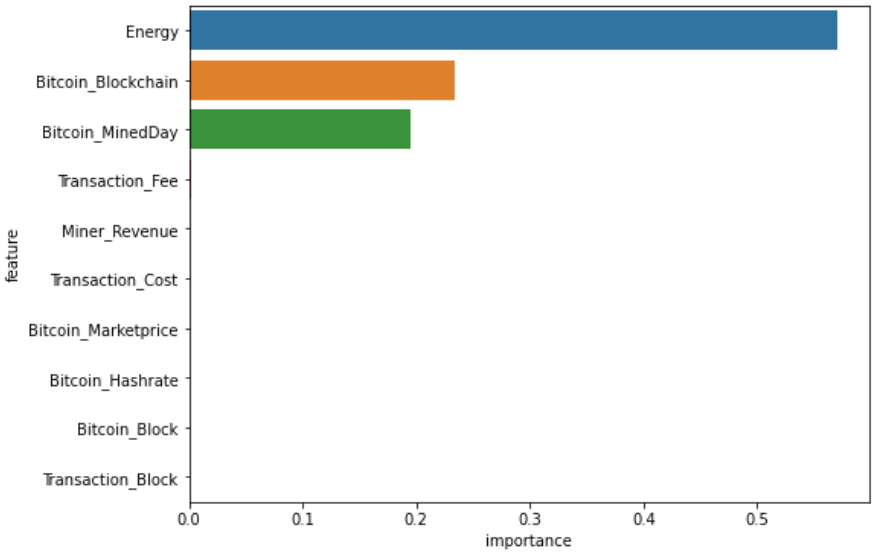

Figure 10. Importance of variables according to GB

Note: Figure 10 exhibits the relative importance of the underlying variables determined by the Gradient Boosting (GB) technique.

Feature importance in GB is determined as per the decreasing node impurity with weight as the probability of reaching the node of constituent regression trees. The node impurity is calculated through mean squared error metrics as the underlying problem is of regression type. The probability value is computed as the ratio of the number of samples reaching the node to the total number of samples. After the computation of the said values, features with higher scores are inferred to be the significant ones. Hence, it is highly likely that the importance scores of underlying features would primarily be driven by the number of occasions they appeared in branching operations of constituent decision trees. A higher appearance in branching operations implies higher predictive ability. In Figure 10, the vertical axis imprints the importance scores of respective features in constructing the GB model. Energy, Bitcoin_Blockchain, and Bitcoin_MinedDay have substantially higher feature importance scores than the remaining ones. This suggests that these three variables appeared predominantly in branching operations and significantly reduced node impurity of most of the constituent regression trees. Therefore, the said approach of ranking feature importance can detect the constructs that largely govern the Ewaste generation. Energy, Bitcoin_Blockchain, and Bitcoin_MinedDay predominantly govern GB modeling. The importance scores of other variables are negligible. These three variables play the most critical role in predicting future movements of electronic waste in the Bitcoin blockchain. Interestingly, they possess a strong association with electronic waste as manifested by MIC and GMIC measures. Thus, the predictive modeling exercise validates the findings of association modeling. So, Energy, Bitcoin_Blockchain, and Bitcoin_MinedDay are the most influential variables. They must be given utmost importance to control the surge in electronic waste.

5. Conclusions

The present research comprehends the statistical properties of the evolutionary patterns of electronic waste generation, decodes the influence of salient independent features pertinent to Bitcoin microstructure, and carries out predictive analytics for forecasting future values of electronic waste. Overall findings of this research reveal critical insights into the electronic waste accumulation process to control its negative impacts. The significant findings of this study are enunciated as follows:

The daily observations of electronic waste generation are strictly non-parametric and non-stationary. Apart from Transaction_Cost and Transaction_Fee, all explanatory features are strictly non-stationary, non-parametric, and driven by fractional Brownian motion. Features pertinent to energy consumption, Bitcoin blockchain size, and the historical number of mined Bitcoins are the most prominent in driving the electronic waste generation process. Thus, any attempt to control waste accumulation must emphasize these factors. Miner revenue shares a comparatively low association. So, a gathering of a large crowd participating in the Bitcoin mining process may not guarantee revenue. However, the crowd's size would increase energy consumption and influence the accumulation of waste in electronic form. All the six machine learning algorithms are highly efficient in carrying out predictive modeling of electronic waste using the said Bitcoin microstructure features. GB is statistically the most superior model, followed by RRF. Predictions by SOM are least accurate.

A steep surge in energy consumption can be controlled by indirectly managing its distribution to other fields (Su et al., 2020). Blockchain is a potential enabler of power distribution across the grids (Upadhyay, 2020). Therefore, developing a robust information system-driven blockchain framework of power management can reduce the footprint of electronic waste. The literature suggests replacing the POW algorithm with a proof-of-stake (POS) mechanism for curbing energy consumption (Li et al., 2019). As the overall energy consumption possesses the utmost influence over electronic waste generations, the present research findings further justify the claim. The economic game-theoretic framework drives POS for maintaining network consensus (Bentov et al., 2014). Under this scheme, network validators must surrender all coins to the network. Any illicit triggering of transactions would result in a complete loss of coins. The amount of archived time and coins will choose validators rewarded with additional coins for validation work. POS is substantially less energy-intensive. Delegated POS (DPOS) and its variant are different promising protocols (Song and Zhao, 2018; Yang et al., 2019) reported to be less energy expensive and can be explored. Alternatively, electronic waste recycling capabilities must be seriously monitored and developed in parallel with exploring renewable energy. The level of ongoing electronic waste accumulation must be appropriately recycled even if there is a viable solution to reduce electronic waste. Thus, critical revamp and innovation of recycling structures across the developed and emerging economies must be emphasized.

In addition to technological innovations and research schemes for handling the arduous task of mitigating the challenge, strategies for curbing the negative effect in framing strict regulations and fiscal policies are of paramount significance. Imposing a tax on revenue over a threshold value may restrain a specific segment of miners from overcrowding the network, thereby results in a viable option for deaccelerating electronic waste growth. This study revealed that the blockchain's size and the number of Bitcoin mined are two significant predictors of waste generation. Proper implementation of these measures can significantly influence controlling such features and eventually lead to great success in reducing the electronic waste work of Truby (2018).

Thus, the outcome of the association mining and the quality of obtained predictions explain the contribution of the present research. The methodology presented in this paper successfully voids the gap in modeling the pattern of electronic waste in the blockchain network of Bitcoin mining. It would be exciting and challenging to examine the nexus and performance of the predictive structure in the presence of additional related variables characterizing the Bitcoin mining process in the blockchain network. In the future, we may test

state-of-the-art deep learning architectures to evaluate their effectiveness in modeling electronic waste and generating insights for control and prevention. The proposed procedure can identify the most significant features based on predictive ability. However, their direction of influence cannot be explicitly determined. In the future, explainable artificial intelligence frameworks may be applied to draw deeper insights.

Acknowledgment

The authors thank the Associate Editor and reviewers for their insightful comments for improving the quality of the paper.

References

Aggarwal, S., Chaudhary, R., Aujla, G.S., Kumar, N., Choo, K.-K.R., Zomaya, A.Y., 2019. Blockchain for smart communities: Applications, challenges and opportunities. J. Netw. Comput. Appl. 144, 13–48.

Atsalakis, G.S., Atsalaki, I.G., Pasiouras, F., Zopounidis, C., 2019. Bitcoin price forecasting with neuro-fuzzy techniques. Eur. J. Oper. Res. 276, 770–780.

Bentov, I., Lee, C., Mizrahi, A., Rosenfeld, M., 2014. Proof of activity: Extending bitcoin's proof of work via proof of stake. ACM SIGMETRICS Perform. Eval. Rev. 42, 34–37.

Cannon, A.J., 2011. Quantile regression neural networks: Implementation in R and application to precipitation downscaling. Comput. Geosci. 37, 1277–1284.

Das, D., Dutta, A., 2020. Bitcoin's energy consumption: Is it the Achilles heel to miner's revenue? Econ. Lett. 186, 1–8. https://doi.org/10.1016/j.econlet.2019.108530

De Vries, A., 2019. Renewable energy will not solve bitcoin's sustainability problem. Joule 3, 893–898.

Deng, H., Runger, G., 2013. Gene selection with guided regularized random forest. Pattern Recognit. 46, 3483–3489.

Di Silvestre, M.L., Gallo, P., Guerrero, J.M., Musca, R., Sanseverino, E.R., Sciumè, G., Vásquez, J.C., Zizzo, G., 2020. Blockchain for power systems: Current trends and future applications. Renew. Sustain. Energy Rev. 119, 109585.

Duong, T.L.V., Thuy, N.T.T., Khai, L.D., 2020. A fast approach for bitcoin blockchain cryptocurrency mining system. Integration 74, 107–114.

Friedman, J.H., 1991. Multivariate adaptive regression splines. Ann. Stat. 1–67.

Ghosh, I., Jana, R.K., Sanyal, M.K., 2019. Analysis of temporal pattern, causal interaction and predictive modeling of financial markets using nonlinear dynamics, econometric models and machine learning algorithms. Appl. Soft Comput. 82, 105553.

Greenberg, P., Bugden, D., 2019. Energy consumption boomtowns in the United States: Community responses to a cryptocurrency boom. Energy Res. Soc. Sci. 50, 162–167.

Islam, A.K.M.N., Mäntymäki, M., Turunen, M., 2019. Why do blockchains split? An actor-network perspective on Bitcoin splits. Technol. Forecast. Soc. Change 148, 119743.

Jana, R.K., Ghosh, I., Sanyal, M.K., 2020. A granular deep learning approach for predicting energy consumption. Appl. Soft Comput. 89, 106091.

Kim, J., Kasabov, N., 1999. HyFIS: adaptive neuro-fuzzy inference systems and their application to nonlinear dynamical systems. Neural Networks 12, 1301–1319.

Kohonen, T., 1982. Self-organized formation of topologically correct feature maps. Biol. Cybern. 43, 59–69.

Kristoufek, L., 2020. Bitcoin and its mining on the equilibrium path. Energy Econ. 85, 104588.

Lally, N., Kay, K., Thatcher, J., 2019. Computational parasites and hydropower: A political ecology of Bitcoin mining on the Columbia River. Environ. Plan. E Nat. Sp. 1–21.

Li, J., Li, N., Peng, J., Cui, H., Wu, Z., 2019. Energy consumption of cryptocurrency mining: A study of electricity consumption in mining cryptocurrencies. Energy 168, 160–168.

Luedtke, A., Tran, L., 2013. The generalized mean information coefficient. arXiv Prepr. arXiv1308.5712.

Nakamoto, S., 2008. Bitcoin: A peer-to-peer electronic cash system.

Reshef, D.N., Reshef, Y.A., Finucane, H.K., Grossman, S.R., McVean, G., Turnbaugh, P.J., Lander, E.S., Mitzenmacher, M., Sabeti, P.C., 2011. Detecting novel associations in large data sets. Science (80-.). 334, 1518–1524.

Schapire, R.E., Singer, Y., 1999. Improved boosting algorithms using confidence-rated predictions. Mach. Learn. 37, 297–336.

Simidjievski, N., Todorovski, L., Džeroski, S., 2015. Predicting long-term population dynamics with bagging and boosting of process-based models. Expert Syst. Appl. 42, 8484–8496.

Song, T.Y., Zhao, Y., 2018. Comparison of blockchain consensus algorithm. Comput. Appl. Softw. 35, 1–8.
Su, C.-W., Qin, M., Tao, R., Umar, M., 2020. Financial implications of fourth industrial revolution: Can bitcoin improve prospects of energy investment? Technol. Forecast. Soc. Change 158, 120178.
Truby, J., 2018. Decarbonizing Bitcoin: Law and policy choices for reducing the energy consumption of Blockchain technologies and digital currencies. Energy Res. Soc. Sci. 44, 399–410.
Upadhyay, N., 2020. Demystifying blockchain: A critical analysis of challenges, applications and opportunities. Int. J. Inf. Manage. 54, 102120.
Yang, F., Zhou, W., Wu, Q., Long, R., Xiong, N.N., Zhou, M., 2019. Delegated proof of stake with downgrade: A secure and efficient blockchain consensus algorithm with downgrade mechanism. IEEE Access 7, 118541–118555.